MAPPING THE

FUTURE OF FLOOD RISK

for the

STILLAGUAMISH &

SNOHOMISH RIVERS

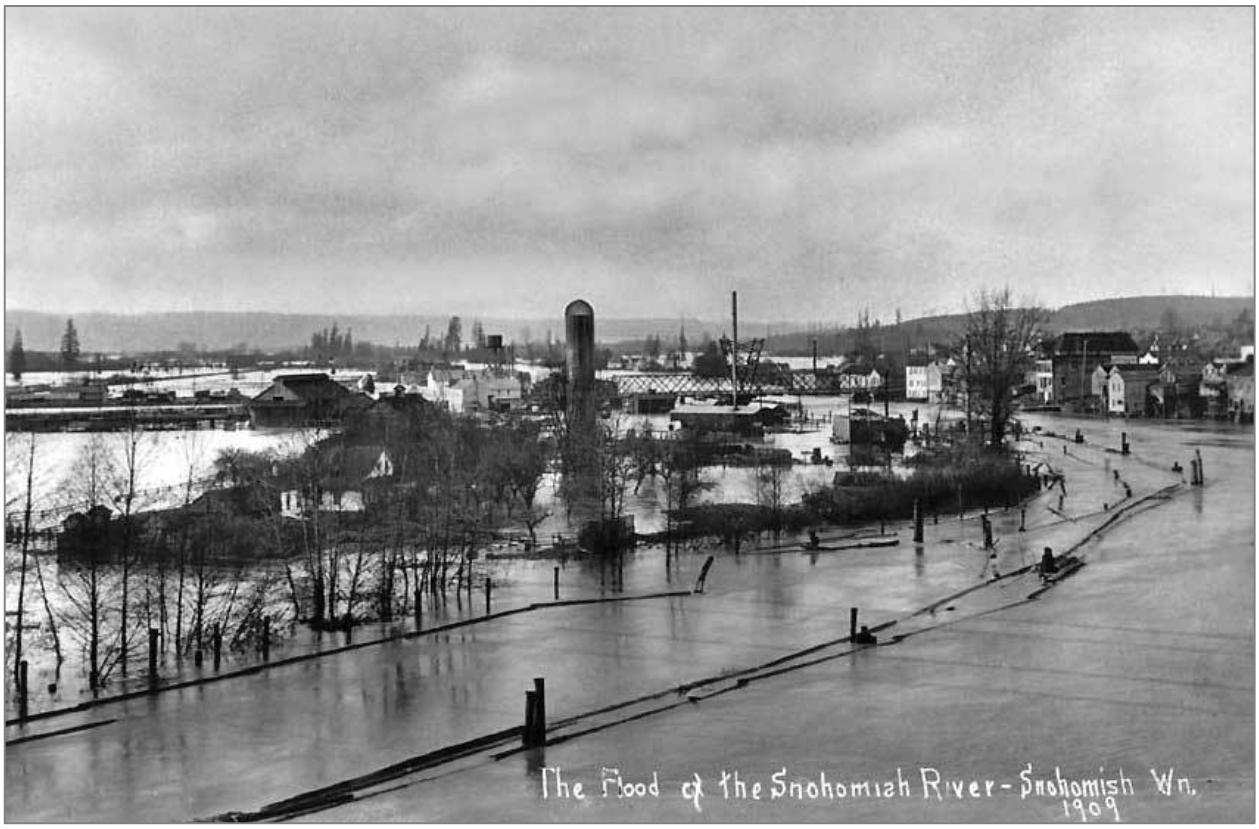

Prepared by the Climate Impacts Group

September 2018 | University of Washington

Guillaume S. Mauger
Se-Yeun Lee
Jason Won

Acknowledgements

The authors would like to thank Jamie Robertson of The Nature Conservancy for his extensive help visualizing the results, providing critical technical review of the findings, and the area tabulations shown in Table 6. We would also like to thank Bart Nijssen and Oriana Chegwidden for their help in using the new Columbia River Climate Change hydrologic projections (CRCC, http://hydro.washington.edu/CRCC/). Sean Crosby, at Western Washington University, provided the storm surge statistics. This project was managed by the Snohomish Conservation District, with funding from the NOAA Community Based Restoration Program, the Estuary and Salmon Restoration Program (Grant #17-1308P), and the Stillaguamish River Lead Entity Capacity Fund.

Cover Image

Image obtained from https://pauldorpat.com/category/washington-then-and-now/

Citation

Mauger, G.S., S.-Y. Lee, J.S. Won, 2018. Mapping the Future of Flood Risk for the Stillaguamish and Snohomish Rivers. Report prepared for the Snohomish Conservation District. Climate Impacts Group, University of Washington, Seattle.

Table of Contents

EXECUTIVE SUMMARY

Climate change is projected to lead to more frequent and severe flooding in response to sea level rise, declining snowpack, and heavier rain events. Most studies of future flood risk have focused on quantifying the amount of sea level rise, or the increase in streamflow during flood events, and have stop short of evaluating which areas are flooded and at what depth. The few studies that have modeled the extent and depth of future flooding (e.g., Hamman et al., 2016; Mauger and Lee, 2014) are limited in spatial coverage and are not easily comparable due to differences in the data and methods used. The purpose of the current project was to pilot a new inexpensive approach to developing a consistent set of flood projections over a much larger area. This allows for apples-to-apples comparisons of risk.

In this study we quantified changes in the depth and extent of flooding for all but the uppermost reaches of the Snohomish and Stillaguamish watersheds. We developed the streamflow and sea level rise projections needed as input to the hydraulic model simulations, in both cases using the latest comprehensive set of projections for the region, and worked with consultants at Fathom, Ltd. (**http://fathom.global/**) to evaluate and optimize the flood simulations. In addition, we evaluated streamflow and sea level rise projections for use in a separate study of groundwater variations in the lower elevations of each basin.

Our projections give a middle estimate of 16-18 inches of sea level rise by the 2080s, and a middle projection showing a +42 to +46% increase in peak streamflow for the 2-year event and -3 to +20% change in the 100-year event. The hydraulic modeling results show a clear increase in flood depth and extent for the more frequent flood events (e.g., 2-year and 10-year); these results are described in a separate report by Fathom, Ltd. (Smith, 2018).

Changes are more ambiguous for the larger events (e.g., 100-year). There are likely two explanations for this: (1) flooding in much of the basin is currently valley wall to valley wall for the 100-year event, meaning that changes in flood extent may be relatively minor for these larger events, and (2) because it is a rare event, it is much more difficult to develop robust statistics for the 100-year event.

Overall, we find strong evidence for an increase in the frequency and extent of flooding for all events, with particularly large changes for the more routine flood events (e.g., 2-year and 10-year). These more frequent flood events are of particular importance for agriculture and ecosystems in each watershed.

TASK 1: SEA LEVEL RISE AND STREAMFLOW PROJECTIONS

We produced projections for two different time periods: the 2050s and 2080s. Each time period refers to an average of the 30-year period centered on that decade (e.g., 2050s = 2040-2069). Since we cannot predict the future of human behavior, we also use two different scenarios of greenhouse gas concentrations (for more on greenhouse gas scenarios, see Section 1 of Mauger et al., 2015). The latest set of greenhouse gas scenarios are called "Representative Concentration Pathways", or RCPs (van Vuuren et al. 2011). In order to bracket the range of future changes, we use both a low (RCP 4.5) and a high (RCP 8.5) scenario of future greenhouse gas concentrations. In order to further account for uncertainty in the projections, we develop low, middle, and high estimates of future change for each time period and scenario. Results are produced for four separate recurrence intervals: the 2-, 10-, 25-

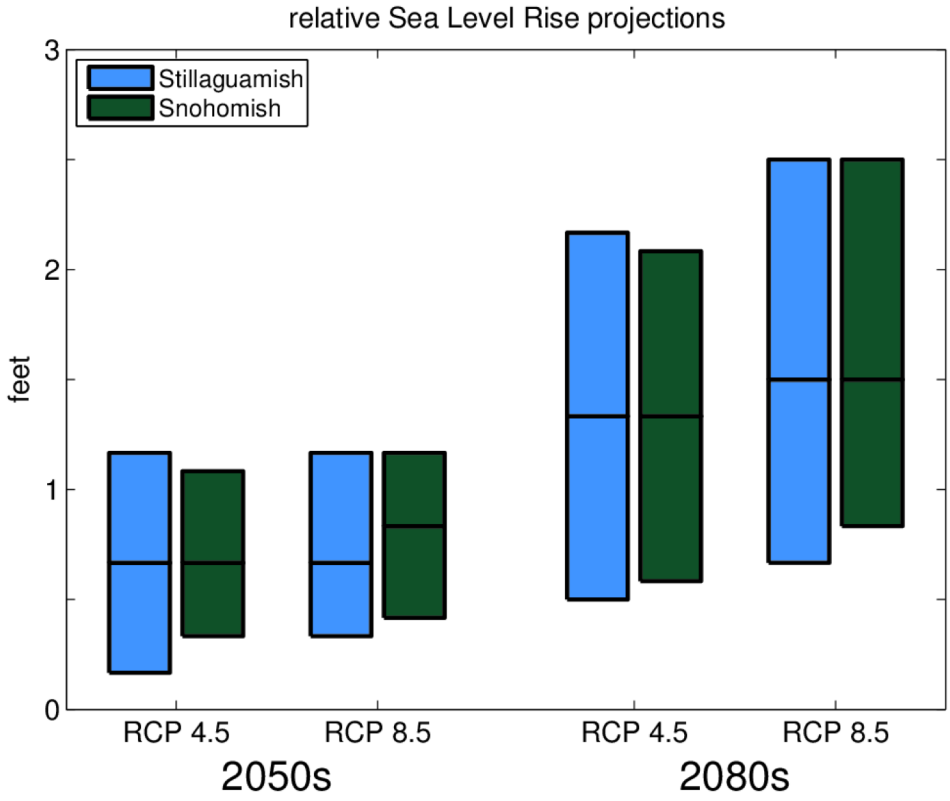

Figure 1. Relative sea level rise projections for the Stillaguamish and Snohomish river deltas. Projections are expressed relative to average sea level for 1990-2010. Results are obtained from Miller et al. (2018) for the two points nearest the outlets of the two Rivers. For each time period and greenhouse gas scenario, a low, middle, and high estimate is provided (specifically: the 5th, 50th, and 95th percentiles, respectively).

, and 100-year flood events. The result is four historical simulations, plus a set of 48 projections of future flood risk (2 time periods x 2 scenarios x 3 projections x 4 recurrence intervals = 48 projections).

Sea Level Rise Projections

A new set of sea level rise projections were recently developed as part of the Washington Coastal Resilience Project (WCRP[1]). Funded via a grant from the NOAA Coastal Resilience program, these projections incorporate the latest science on global and regional sea level rise, while accounting for the local effects of vertical land motion, since it is the change in sea level relative to land that determines impacts (Miller et al., 2018). We extracted projections for this new dataset for two points that are close to the mouth of each river (**Figure 1, Table 1**). In order to assess the range among projections, we included a low, middle, and high estimate for each scenario and time period. These correspond to the 5th, 50th, and 95th percentile estimates in each instance.

			2050s						2080s					
			RCP 4.5 (Low)			RCP 8.5 (High)			RCP 4.5 (Low)			RCP 8.5 (High)		
River Delta	**Lat.**	**Long.**	**low**	**mid**	**hgh**	**low**	**mid**	**hgh**	**low**	**mid**	**hgh**	**low**	**mid**	**hgh**
Stillaguamish	*48.2N*	*122.4W*	2	8	14	4	8	14	6	16	26	8	18	30
Snohomish	*48.0N*	*122.2W*	4	8	13	5	10	14	7	16	25	10	18	30

Table 1. Relative sea level rise projections, as shown in Figure 1. Projections are expressed in inches, relative to the average for 1990-2010. Results were obtained from Miller et al. (2018) for the two points nearest the outlets of the Snohomish and Stillaguamish Rivers. For each time period and greenhouse gas scenario, a low, middle, and high estimate is provided.

Sea level rise will lead to greater storm surge impacts, simply because a higher sea level translates to higher water levels during storm events. However, there is currently no evidence that the amount of storm surge itself will increase in the future – studies to date have not found a trend in the intensity of winds during storm events, for example (Salathé et al., 2015). As a result, we use the same storm surge estimate for both our historical and future simulations. These are added to the base sea level in each instance: current sea level for the historical simulations, and projected sea level for the future simulations.

Storm surge was estimated for each river delta using tide gauge records at Priest Point and Tulare Beach (**Figure 2, Table 2**). Although Priest Point is right at the mouth of the Snohomish River, Tulare Beach is about 5 miles to the south of the Stillaguamish River delta. Surge estimates were developed by taking the tidal predictions at each tide gauge (astronomical tides resulting from the gravitational pull of the sun and moon) and adding the tidal "anomalies" (difference between observed and

[1] http://www.wacoastalnetwork.com/washington-coastal-resilience-project.html

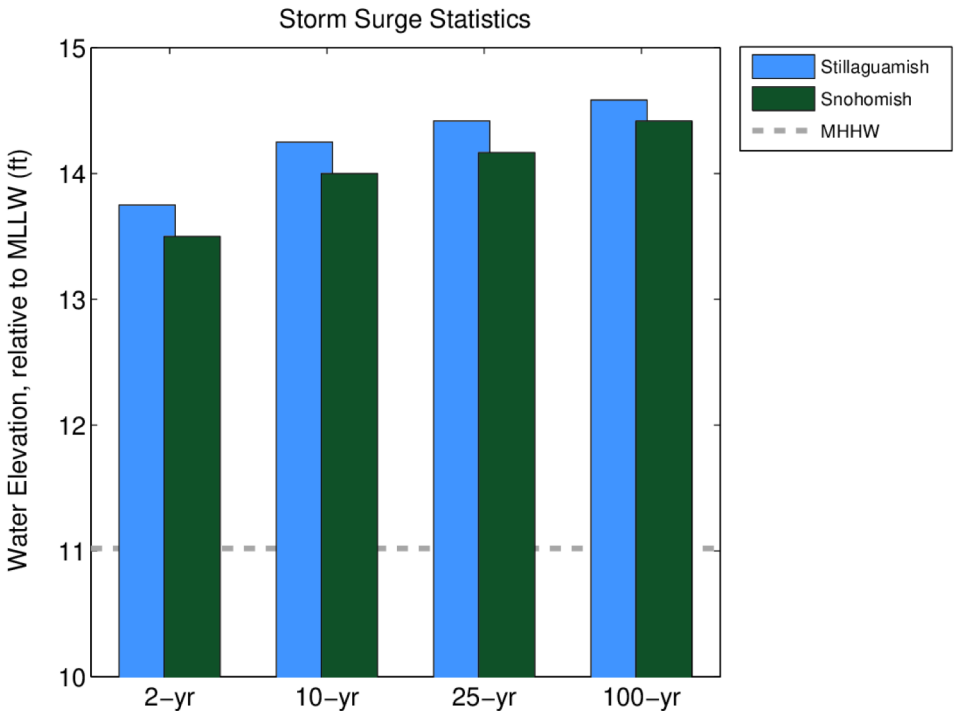

Figure 2. Storm surge statistics for the Stillaguamish and Snohomish river deltas. Results were obtained from Sean Crosby at Western Washington University (WWU). All values are expressed relative to Mean Lower Low Water (MLLW). For reference, the grey dashed line shows the elevation for Mean Higher High Water (MHHW).

predicted tide) for the four longest-running stations in Puget Sound (Seattle, Friday Harbor, Port Townsend, Cherry Point). Tidal anomalies are a measure of storm surge, as measured by tide gauges (Sean Crosby, personal communication). Recent analyses suggest that the tidal anomaly statistics are the same for all gauges in Puget Sound; by using the longest tide gauges in the region we are able to obtain more reliable statistics of the likelihood of extreme storm surge. Combining the tidal anomalies with the tidal predictions gives a time series for total water levels, which were then fit to a Generalized Extreme Value distribution to obtain the extreme statistics shown in Table 2.

		Recurrence Interval			
River Delta	**Tide Gauge**	**2-yr**	**10-yr**	**25-yr**	**100-yr**
Stillaguamish	*Tulare Beach*	165	171	173	175
Snohomish	*Priest Point*	162	168	170	173

Table 2. Storm surge statistics, as shown in Figure 2. All values are expressed relative to Mean Lower Low Water (MLLW), in inches.

Peak Streamflow Projections

Streamflow projections were obtained from the forthcoming River Management Joint Operating Committee, Phase II effort (RMJOC-II, 2018), led by UW colleague Bart Nijssen. This new dataset includes substantial improvements in both the climate drivers and the hydrologic modeling used as a basis for the projections. Runoff from the model was routed to produce streamflow estimates at a total of 154 hydrodynamic model input points (Table A1; see Figure 6 in Fathom, 2018). In addition, streamflow estimates were produced for a few sites for use in a parallel effort aimed at modeling groundwater variations (Table 3).

Site Name	USGS ID
Stillaguamish River Near Stanwood	12170050
NF Stillaguamish River Near Arlington	12167000
Snohomish River at Snohomish	12155500
Snohomish River Near Monroe	12150800
Skagit River Near Mt Vernon	12200500

Table 3. Streamflow sites used in groundwater modeling. As in Table A1, historical and future routed flows were produced for these sites using the projections from the RMJOC-II dataset.

Streamflow Routing

The hydrologic model projections from RMJOC-II provide gridded estimates of surface runoff and sub-surface flows on a 1/16-degree (about 5 x 7 km) model grid. Since any particular streamflow site may contain multiple grid cells within its catchment area, an additional step is needed to estimate total streamflow at each location. This process is referred to as streamflow "routing", because flows are routed through the stream network. In this project, we obtained projections from the RMJOC-II dataset, then routed flows for each of the streamflow points listed in Table A1 and Table 3.

To perform the routing, we used the simulated surface and sub-surface flows from each grid cell (sometimes referred to as runoff and baseflow, respectively) as input to a daily-time-step routing model developed by Lohmann et al. (1996). The within-cell routing uses a "Unit Hydrograph" approach to represent the temporal distribution of flow at the outlet point from an impulse input at each source point. The channel routing uses the linearized Saint-Venant equation to represent the flow at a downstream point as a function of the water velocity and the diffusivity, both of which may be estimated from geographical data (Lohmann et al., 1998). The river routing model assumes all runoff and baseflow exit a cell in a single flow direction.

A predetermined routing network provides the upstream-downstream linkage between model grid cells. All sites in Table A1 and Table 3 were then located on the developed streamflow routing network

and verified based on their true latitude-longitude location, the cited watershed area by the USGS and the World Hydro Reference Overlay Map showing flow of the rivers.

Extreme Statistics

Once daily streamflow estimates have been obtained at each site, an additional step is needed to estimate daily streamflow extremes. To calculate extreme statistics, we applied the GEV distribution with L-moments – following the methodology described in Salathé et al. (2014) and Tohver et al. (2014). These distributions are selected based on findings that indicate it is superior to the LP3 distribution (Rahman et al., 1999, 2015; Vogal et al., 1993; Nick et al., 2011). Flood flows were computed for return intervals of 2, 10, 25, and 100 years (50%, 10%, 4%, and 1% exceedance values). To estimate flood magnitude, the maximum daily flows were extracted for each water year (October to September) at each site. These were ranked for each 30-year period and fitted to the GEV with L-moments (Wang, 1997; Hosking and Wallis, 1993; Hosking, 1990).

Conversion to Peak Discharge

Since the modeled streamflow estimates may be biased high or low relative to the observation, only the percent change in peak flow statistics was taken from the streamflow projections. These were then used to scale the historical peak flow statistics that were developed by Fathom. Fathom used a regionalization, based on observed gauge data, to relate peak flow statistics to basin area (Fathom, 2018). Prior results (WEST, 2001) indicate that the gauge record may under-represent the magnitude of larger floods, given several large floods that occurred in the late 1800s. To account for this, Fathom used the 90th percentile estimates of the best fit parameters for the GEV distribution to estimate the magnitude of the extreme statistics. The result is a set of historical and future peak discharge estimates (e.g., in CFS or ft^3/s), for each of the model boundary points (Table A1), for use as inputs to the hydrodynamic model.

Results

Projected changes in streamflow statistics are summarized in **Figure 3 and Table 4**. For simplicity, we provide the average change among all sites listed in Table A1; results for each model boundary point are provided in a separate document. Nearly all projections indicate an increase in peak flows across all time periods, scenarios, and return intervals. Projected changes are generally larger for the 2080s than the 2050s, and the middle projections show a large difference between the two greenhouse gas scenarios for the 2080s. The results also suggest that the changes are largest for the 2-year peak flow discharge and smallest for the 100-year event.

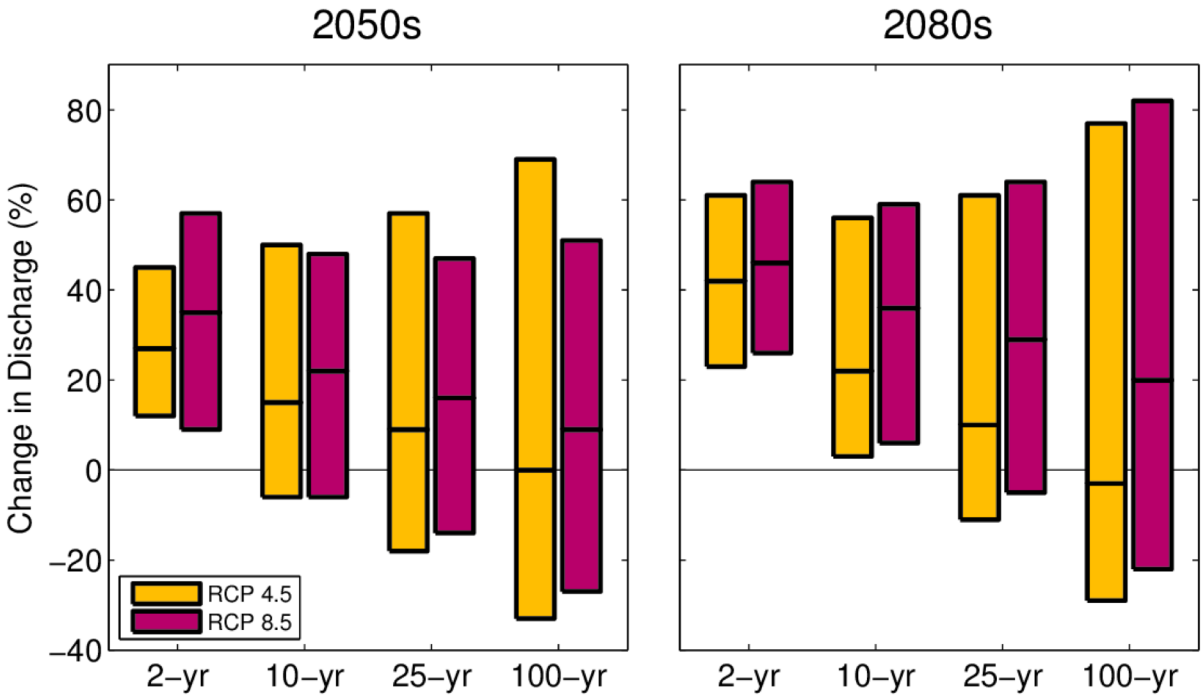

Figure 3. Percent (%) change in peak river flow (discharge) statistics, relative to the average for 1970-1999. Results show the average change, obtained from RMJOC (2018), among all sites listed in Table A1. For each time period and greenhouse gas scenario, a low, middle, and high estimate is provided. Statistics are based on maximum in daily average streamflow for each water year.

In general, we expect flood risk to increase in the future, due to a combination of decreased snowpack and more intense heavy rains. There are, however, some projections that indicate a decrease in peak flows in the future. This is likely due to a combination of several factors: (1) some models show a lower sensitivity to greenhouse gases, resulting in a smaller increase in peak flows, (2) although most models indicate an increase in the intensity of heavy rain events, there are a few that project a decrease, and (3) random fluctuations associated with natural variability can cause peak flows to temporarily decrease, even if the long-term trend indicates an increase in peak flows.

	2050s						2080s					
	RCP 4.5 (Low)			RCP 8.5 (High)			RCP 4.5 (Low)			RCP 8.5 (High)		
Return Freq.	**low**	**mid**	**hgh**	**low**	**mid**	**hgh**	**low**	**mid**	**hgh**	**low**	**mid**	**hgh**
2-year	12	27	45	9	35	57	23	42	61	26	46	64
10-year	-6	15	50	-6	22	48	3	22	56	6	36	59
25-year	-18	9	57	-14	16	47	-11	10	61	-5	29	64
100-year	-33	0	69	-27	9	51	-29	-3	77	-22	20	82

Table 4. Percent (%) change in peak river flow (discharge) statistics, as shown in Figure 3.

Given the robust decreases in snowpack that are expected with climate change, the only way that flood risk can decrease is if there is a compensating decrease in the intensity of heavy rain events. The projected decreases in Table 4 are most pronounced for the 100-year event and nonexistent for the 2-year event. This suggests that the third explanation – natural variability – plays a large role in determining the changes for each time period. We have confirmed this by using a longer time period to evaluate changes: by comparing peak flow statistics for 50-year instead of 30-year periods (1950-1999 vs. 2050-2099), we reduce the influence of short-term fluctuations. With these new calculations, a much smaller number of models project a decrease in peak flow extremes, confirming that the primary explanation for the decreases shown in Table 4 is a result of random natural variability.

Since many managers monitor river stage as opposed to discharge, we have converted the changes in discharge to the corresponding river stage at the two commonly-used gauges (NF Stillaguamish near Arlington, USGS #12167000; and Snohomish near Monroe, USGS #12150800; **Table 5**).

			2050s						2080s					
			RCP 4.5 (Low)			RCP 8.5 (High)			RCP 4.5 (Low)			RCP 8.5 (High)		
	Return Freq.	Hist	low	mid	hgh	low	mid	hgh	low	mid	hgh	low	mid	hgh
Stillaguamish	*2-year*	2.5	2.5	2.6	2.8	2.5	2.7	2.8	2.6	2.7	2.9	2.6	2.7	2.9
	10-year	3.2	3.1	3.3	3.8	3.2	3.4	3.5	3.2	3.4	3.7	3.3	3.5	3.8
	25-year	3.6	3.4	3.7	4.3	3.5	3.7	3.9	3.4	3.7	4.2	3.6	3.9	4.2
	100-year	4.2	3.8	4.3	5.2	3.9	4.3	4.7	3.8	4.1	5.3	4.0	4.5	5.1
Snohomish	*2-year*	1.2	1.5	1.7	1.9	1.4	1.8	2.0	1.6	1.9	2.1	1.7	2.0	2.1
	10-year	2.2	2.0	2.4	3.0	2.1	2.5	2.9	2.3	2.5	2.9	2.3	2.8	3.1
	25-year	2.8	2.2	2.9	4.0	2.3	2.9	3.7	2.5	2.9	3.5	2.7	3.3	4.0
	100-year	3.7	2.2	3.3	5.4	2.5	3.2	4.9	2.5	3.1	4.3	2.8	3.7	5.1

Table 5. Historical and projected river stage (ft) estimates used in the current study. Results are shown for the model boundary points nearest the North Fork Stillaguamish River near Arlington (USGS #12167000: Qin_18_1_792.0233) and the Snohomish River near Monroe (USGS #12150800: sum of Qin_11_1_1756.391 and Qin_12_1_1759.2578), and are based on the stage-discharge relationship published by USGS (Dated April 4th, 2018; Accessed on June 6th, 2018).

TASK 2: FLOOD MODELING

We worked with Fathom, Ltd. to support the application of their model to the Stillaguamish and Snohomish river basins, providing sea level rise and streamflow projections described in the previous section. Snohomish Conservation District, Snohomish County, and others provided a fine-scale DEM for model development as well as feedback during model testing and development. All of the details for the model development, testing, and results are described in a companion report produced by Fathom, Ltd. (Smith, 2018). **Figure 4**, along with **Tables 6 and 7**, provide a brief overview of the results; additional details can be obtained by browsing The Nature Conservancy's Coastal Resilience web tool:

http://maps.coastalresilience.org/washington/

The vast majority of the results show an increase in flood risk, and that this increase is greater for higher greenhouse gas emissions. However, as in the streamflow projections, a few projections

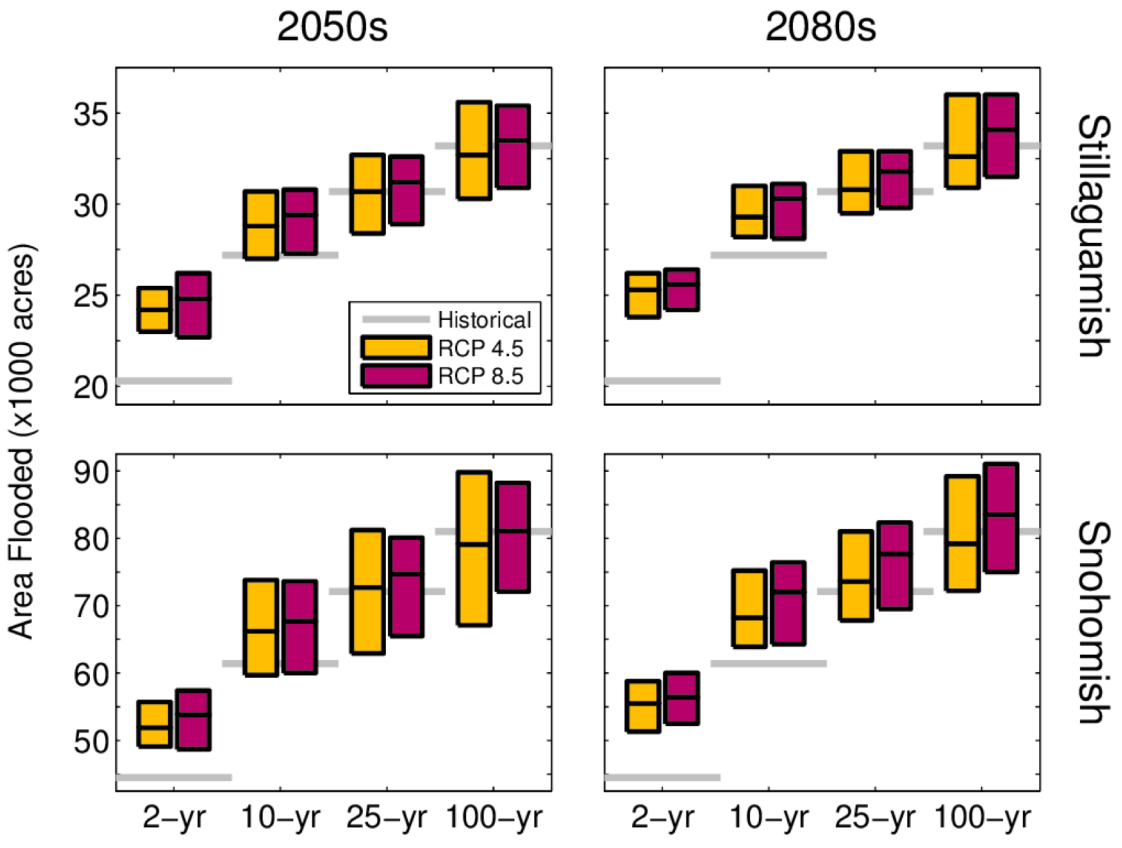

Figure 4. Total area flooded (in thousands of acres) for the Snohomish and Stillaguamish watersheds. For each time period and greenhouse gas scenario, a low, middle, and high estimate is provided, all based on the flood simulations produced by Fathom.

indicate a decrease in flood risk. In addition to the two explanations described above, there is an additional factor that may affect the sensitivity to climate change for large events: In the Stillaguamish and Snohomish river basins, large floods often extend from valley wall to valley wall. In these areas, changes in the area flooded will be minimal, resulting in very little apparent change in flood risk.

			2050s						2080s					
			RCP 4.5 (Low)			RCP 8.5 (High)			RCP 4.5 (Low)			RCP 8.5 (High)		
	Return Freq.	Hist.	low	mid	hgh	low	mid	hgh	low	mid	hgh	low	mid	hgh
Stillaguamish	*2-year*	20300	23000	24200	25400	22700	24800	26200	23800	25300	26200	24200	25600	26400
	10-year	27200	27000	28800	30700	27300	29400	30800	28200	29300	31000	28100	30300	31100
	25-year	30700	28400	30700	32700	28900	31200	32600	29500	30800	32900	29800	31800	32900
	100-year	33200	30300	32700	35600	30900	33500	35400	30900	32600	36000	31500	34100	36000
Snohomish	*2-year*	44500	49100	51900	55700	48700	53800	57400	51300	55500	58800	52500	56400	60000
	10-year	61400	59700	66200	73800	60000	67700	73600	63900	68200	75200	64300	72000	76400
	25-year	72100	62900	72700	81200	65500	74700	80100	67800	73600	81000	69500	77700	82300
	100-year	81000	67100	79100	89800	72100	81100	88200	72200	79200	89200	75000	83500	91000

Table 6. Total area flooded (in acres) for the Snohomish and Stillaguamish watersheds. For each time period and greenhouse gas scenario, a low, middle, and high estimate is provided, all based on the flood simulations produced by Fathom.

		2050s						2080s					
		RCP 4.5 (Low)			RCP 8.5 (High)			RCP 4.5 (Low)			RCP 8.5 (High)		
	Return Freq.	low	mid	hgh	low	mid	hgh	low	mid	hgh	low	mid	hgh
Stillaguamish	*2-year*	13	19	25	12	22	29	17	25	29	19	26	30
	10-year	-1	6	13	0	8	13	4	8	14	3	11	14
	25-year	-7	0	7	-6	2	6	-4	0	7	-3	4	7
	100-year	-9	-2	7	-7	1	7	-7	-2	8	-5	3	8
Snohomish	*2-year*	10	17	25	9	21	29	15	25	32	18	27	35
	10-year	-3	8	20	-2	10	20	4	11	22	5	17	24
	25-year	-13	1	13	-9	4	11	-6	2	12	-4	8	14
	100-year	-17	-2	11	-11	0	9	-11	-2	10	-7	3	12

Table 7. As in Table 6, except showing the percent change in area flooded.

REFERENCES

Hamman, J. J., Hamlet, A. F., Lee, S. Y., Fuller, R., & Grossman, E. E. (2016). Combined Effects of Projected Sea Level Rise, Storm Surge, and Peak River Flows on Water Levels in the Skagit Floodplain. Northwest Science, 90(1), 57-78.

Hosking, J. R. M., & Wallis, J. R. (1993). Some statistics useful in regional frequency analysis. Water Resources Research, 29(2), 271-281.

Hosking, J.R.M., 1990. L-moments: analysis and estimation of distributions using linear combinations of order statistics. Journal of the Royal Statistical Society, Series B, 52,105-124.

Lohmann, D., R. Nolte-Holube, and E. Raschke, 1996: A large-scale horizontal routing model to be coupled to land surface parametrization schemes, Tellus, 48(A), 708-721.

Lohmann, D., E. Raschke, B. Nijssen and D. P. Lettenmaier, 1998: Regional scale hydrology: I. Formulation of the VIC-2L model coupled to a routing model, Hydrol. Sci. J., 43(1), 131-141.

Mauger, G. S., and S.-Y. Lee, 2014. Climate Change, Sea Level Rise, and Flooding in the Lower Snohomish River Basin. Report prepared for The Nature Conservancy by the Climate Impacts Group, University of Washington, Seattle.

Mauger, G.S., J.H. Casola, H.A. Morgan, R.L. Strauch, B. Jones, B. Curry, T.M. Busch Isaksen, L. Whitely Binder, M.B. Krosby, and A.K. Snover, 2015. State of Knowledge: Climate Change in Puget Sound. Report prepared for the Puget Sound Partnership and the National Oceanic and Atmospheric Administration. Climate Impacts Group, University of Washington, Seattle. **https://doi.org/10.7915/CIG93777D**

Nick, M., Das, S. and Simonovic, S.P. 2011. The Comparison of GEV, Log-Pearson Type 3 and Gumbel Distributions in the Upper Thames River Watershed under Global Climate Models, the University of Western Ontario Department of Civil and Environmental Engineering, Report No:077.

Rahman, A., Karin, F, and Rahman, A. 2015. Sampling Variability in Flood Frequency Analysis: How Important is it? 21st International Congress on Modelling and Simulation, Gold Coast, Australia, Nov 29-Dec 4, 2015, 2200-2206.

Rahman, A., Weinmann, P.E. and Mein, R.G. (1999). At-site flood frequency analysis: LP3-product moment, GEV-L moment and GEV-LH moment procedures compared. In: Proceeding Hydrology and Water Resource Symposium, Brisbane, 6–8 July, 2, 715–720.

River Management Joint Operating Committee (RMJOC), 2018: Climate and Hydrology Datasets for RMJOC Long-Term Planning Studies, Second Edition: Part I – Hydroclimate Projections and Analyses. 112pp. Available on line at: **https://www.bpa.gov/p/Generation/Hydro/Pages/Climate-Change-FCRPS-Hydro.aspx**

Salathé Jr, E. P., Hamlet, A. F., Mass, C. F., Lee, S. Y., Stumbaugh, M., & Steed, R. (2014). Estimates of 21st century flood risk in the Pacific Northwest based on regional climate model simulations. Journal of Hydrometeorology, (2014).

Smith, A. (2018). *Puget Sound Hazard Mapping Report.* Report prepared for The Snohomish Conservation District by Fathom, Ltd.

Tohver, I. M., Hamlet, A. F., & Lee, S. Y. (2014). Impacts of 21st‐Century Climate Change on Hydrologic Extremes in the Pacific Northwest Region of North America. JAWRA Journal of the American Water Resources Association, 50(6), 1461-1476.

Van Vuuren, D., J. Edmonds, M. Kainuma, K. Riahi, A. Thomson, K. Hibbard, G. Hurtt, T. Kram, V. Krey, J. Lamarque, T. Masui, M. Meinshausen, N. Nakicenovic, S. Smith, S. Rose, 2011: The representative concentration pathways: an overview. Climatic Change, 109: 5-31. **http://dx.doi.org/10.1007/s10584-011-0148-z**

Vogel, R.M., McMahon, T.A. and Chiew, F.H.S. (1993). Flood flow frequency model selection in Australia, Journal Hydrology, 146, 421-449.

Wang, Q.J. 1997. LH moments for statistical analysis of extreme events. Water Resour Res, 33(12), 2841-2848.

WEST Consultants, Inc. (WEST), (2001). Technical Support Data Notebook for Snohomish County, City of Everett, City of Marysville, City of Snohomish, and Unincorporated Areas, Restudy Flood Insurance Study, prepared for Seattle District, Corps of Engineers, and FEMA Region 10, April 2001.

APPENDIX A

Table A1. Model boundary points for the hydraulic model. Streamflow projections were provided to Fathom for each of these points, distributed across the Snohomish and Stillaguamish river basins. Due to the relatively coarse spatial resolution of the VIC hydrologic model, some sites are located within the same grid cell. In these cases, the same projections were provided for each site.

ID	Long	Lat	VIC Long	VIC_Lat	Notes
SN208	-121.38708	47.91875	-121.34375	47.96875	Same as Qin_21_1_218.3225
SN200	-121.45375	47.50458	-121.40625	47.46875	Upstream of Qin_7_1_861.9765
SN206	-121.48792	47.58375	-121.46875	47.59375	Upstream of Qin_16_1_603.8715
SN204	-121.50458	47.39542	-121.46875	47.40625	Upstream of Qin_13_1_1023.8802
SN207	-121.53208	47.46125	-121.53125	47.46875	Same as Qin_24_1_796.2526 and Qin_17_1_903.2416
SN210	-121.57792	48.07542	-121.53125	48.09375	Upstream of Qin_24_1_766.3286
SN203	-121.62125	47.66292	-121.59375	47.65625	Upstream of Qin_12_1_1360.1205
SN212	-121.62792	48.21292	-121.65625	48.15625	Same as Qin_27_1_418.85773
SN205	-121.62958	47.70458	-121.59375	47.71875	Same as Qin_15_1_707.5738
SN202	-121.63792	47.74792	-121.59375	47.78125	Same as Qin_10_1_841.4386
SN209	-121.63792	48.40458	-121.65625	48.40625	Same as Qin_23_1_439.4818
SN211	-121.73042	48.14542	-121.71875	48.15625	Same as Qin_26_1_507.4592
SN201	-121.79625	48.01292	-121.78125	48.03125	Upstream of Qin_8_1_427.6026
FOSSR	-121.29800	47.69700	-121.28125	47.65625	This point is not included in the model boundary points
TYERR	-121.22600	47.71600	-121.21875	47.71875	This point is not included in the model boundary points
Qin_10_1_841.4386	-121.66292	47.74792	-121.59375	47.78125	
Qin_11_1_1756.391	-122.00375	47.82625	-121.96875	47.84375	
Qin_11_1_540.1737	-121.53792	47.99625	-121.46875	47.96875	
Qin_6_1_706.0495	-121.33764	47.72931	-121.28125	47.78125	Qin_11_1_579.5937 is in the same VIC location as Qin_6_1_706.0495
Qin_11_1_579.5937	-121.33764	47.72097	-121.28125	47.78125	Qin_11_1_579.5937 is in the same VIC location as Qin_6_1_706.0495

ID	Long	Lat	VIC Long	VIC_Lat	Notes
Qin_12_1_1360.1205	-121.68125	47.64125	-121.65625	47.65625	
Qin_12_1_1465.2294	-121.57208	47.53708	-121.53125	47.53125	
Qin_12_1_1759.2578	-122.00625	47.81125	-121.96875	47.78125	
Qin_13_1_1023.8802	-121.57542	47.40875	-121.53125	47.40625	
Qin_13_1_201.2834	-122.08792	47.90375	-122.09375	47.96875	
Qin_13_1_255.6953	-121.93042	48.02958	-121.65625	48.03125	
Qin_14_1_38.573	-122.19708	48.03708	-122.15625	48.09375	Qin_14_1_38.573 and Qin_21_1_23.6492 are in the same VIC location
Qin_21_1_23.6492	-122.17125	48.08792	-122.15625	48.09375	Qin_14_1_38.573 and Qin_21_1_23.6492 are in the same VIC location
Qin_14_1_639.1412	-121.41292	47.89708	-121.40625	47.90625	
Qin_14_1_716.8899	-121.38042	47.60375	-121.40625	47.59375	
Qin_15_1_632.6853	-121.72708	47.72542	-121.65625	47.78125	
Qin_15_1_707.5738	-121.65458	47.70125	-121.59375	47.71875	
Qin_16_1_2115.4603	-121.80542	47.86125	-121.78125	47.84375	
Qin_16_1_337.5873	-121.57875	47.97875	-121.53125	47.96875	
Qin_16_1_603.8715	-121.53625	47.55625	-121.53125	47.59375	
Qin_16_1_904.5067	-121.38208	47.71792	-121.34375	47.71875	
Qin_17_1_1326.5529	-121.70458	47.47958	-121.65625	47.46875	
Qin_17_1_1496.9986	-121.56292	47.80375	-121.53125	47.78125	
Qin_17_1_1574.0317	-121.71708	47.58125	-121.71875	47.59375	
Qin_17_1_2182.1383	-121.92958	47.62125	-121.90625	47.59375	
Qin_24_1_796.2526	-121.58125	47.51958	-121.53125	47.46875	Qin_24_1_796.2526 is in the same VIC location as Qin_17_1_903.2416
Qin_17_1_903.2416	-121.54292	47.47542	-121.53125	47.46875	Qin_24_1_796.2526 is in the same VIC location as Qin_17_1_903.2416
Qin_18_1_1176.9253	-121.63792	47.43292	-121.59375	47.40625	
Qin_18_1_226.7187	-122.01125	48.06958	-121.96875	48.03125	
Qin_18_1_2576.992	-121.82042	47.52958	-121.78125	47.53125	
Qin_18_1_309.4336	-122.06375	47.96625	-122.03125	47.96875	
Qin_18_1_454.5499	-121.62125	47.94625	-121.59375	47.90625	

ID	Long	Lat	VIC Long	VIC_Lat	Notes
Qin_18_1_792.0233	-122.11458	48.21458	-122.03125	48.28125	
Qin_19_1_225.8208	-122.03042	48.01292	-122.03125	48.03125	
Qin_19_1_485.9549	-121.41125	47.66042	-121.46875	47.65625	
Qin_19_1_57.1763	-121.97208	47.97958	-121.96875	47.96875	Qin_19_1_57.1763, Qin_24_1_69.4108, and Qin_24_1_92.3145 are in the same VIC location
Qin_24_1_69.4108	-121.91875	47.91625	-121.96875	47.96875	Qin_19_1_57.1763, Qin_24_1_69.4108, and Qin_24_1_92.3145 are in the same VIC location
Qin_24_1_92.3145	-121.96208	47.95792	-121.96875	47.96875	Qin_19_1_57.1763, Qin_24_1_69.4108, and Qin_24_1_92.3145 are in the same VIC location
Qin_19_1_721.2054	-122.11292	48.20458	-122.09375	48.15625	
Qin_19_1_891.9203	-121.91958	47.63708	-121.84375	47.65625	
Qin_19_1_895.1746	-121.47042	47.87042	-121.46875	47.90625	
Qin_20_1_117.3021	-122.22042	48.21208	-122.21875	48.28125	Qin_20_1_117.3021 is in the same VIC location as Qin_31_1_180.7493
Qin_31_1_180.7493	-122.17958	48.25792	-122.21875	48.28125	Qin_20_1_117.3021 is in the same VIC location as Qin_31_1_180.7493
Qin_20_1_354.3487	-121.58875	48.00458	-121.59375	48.03125	Qin_32_1_213.2453 is in the same VIC location as Qin_20_1_354.3487
Qin_32_1_213.2453	-121.59708	47.98875	-121.59375	48.03125	Qin_32_1_213.2453 is in the same VIC location as Qin_20_1_354.3487
Qin_20_1_448.7082	-121.37292	47.65458	-121.34375	47.65625	
Qin_20_1_449.5187	-121.79375	47.71125	-121.71875	47.78125	
Qin_20_1_723.1392	-121.82458	47.86542	-121.78125	47.90625	
Qin_20_1_864.9407	-121.56375	47.81625	-121.53125	47.84375	
Qin_21_1_1344.9244	-121.86958	47.66125	-121.84375	47.71875	
Qin_21_1_218.3225	-121.39625	47.90458	-121.34375	47.96875	
Qin_21_1_319.2059	-121.78792	47.62875	-121.78125	47.65625	
Qin_21_1_808.464	-121.66542	47.97458	-121.65625	47.96875	
Qin_22_1_1074.7162	-121.76708	47.52375	-121.71875	47.53125	
Qin_22_1_110.8328	-121.93792	47.86625	-121.90625	47.90625	
Qin_22_1_514.3431	-121.88042	47.48708	-121.90625	47.46875	Qin_22_1_514.3431 is in the same VIC location as Qin_27_1_463.1391
Qin_27_1_463.1391	-121.92042	47.51458	-121.90625	47.46875	Qin_22_1_514.3431 is in the same VIC location as Qin_27_1_463.1391

ID	Long	Lat	VIC Long	VIC_Lat	Notes
Qin_22_1_855.8116	-121.79792	47.93125	-121.78125	47.96875	
Qin_23_1_101.0969	-121.96208	47.76375	-121.90625	47.78125	Qin_23_1_101.0969, Qin_27_1_154.873, Qin_29_1_170.5893 are in the same VIC location
Qin_27_1_154.873	-121.91125	47.74292	-121.90625	47.78125	Qin_23_1_101.0969, Qin_27_1_154.873, Qin_29_1_170.5893 are in the same VIC location
Qin_29_1_170.5893	-121.88042	47.76375	-121.90625	47.78125	Qin_23_1_101.0969, Qin_27_1_154.873, Qin_29_1_170.5893 are in the same VIC location
Qin_23_1_23.8558	-122.16208	48.11958	-122.15625	48.15625	
Qin_23_1_439.4818	-121.61958	48.35292	-121.65625	48.40625	
Qin_23_1_731.1964	-121.72125	47.68958	-121.65625	47.71875	
Qin_23_1_803.5802	-121.72958	47.46875	-121.65625	47.40625	
Qin_24_1_26.5766	-122.34375	48.33875	-122.28125	48.34375	Outside of the Snohomish River. Part of the Skagit River basin.
Qin_24_1_49.1174	-122.06958	47.90625	-122.03125	47.90625	
Qin_24_1_766.3286	-121.63958	48.06458	-121.59375	48.09375	
Qin_25_1_207.2506	-121.91708	47.62375	-121.84375	47.59375	Qin_26_1_289.9447 is in the same VIC location as Qin_25_1_207.2506
Qin_26_1_289.9447	-121.84375	47.62125	-121.84375	47.59375	Qin_26_1_289.9447 is in the same VIC location as Qin_25_1_207.2506
Qin_25_1_22.8963	-122.31208	48.24458	-122.34375	48.28125	Qin_25_1_22.8963 and Qin_42_1_21.4344 are in the same VIC location
Qin_42_1_21.4344	-122.30708	48.25458	-122.34375	48.28125	Qin_25_1_22.8963 and Qin_42_1_21.4344 are in the same VIC location
Qin_25_1_28.0969	-122.19708	48.03375	-122.15625	48.03125	
Qin_25_1_293.3251	-121.72958	47.92792	-121.71875	47.90625	Qin_28_1_270.358, Qin_25_1_293.3251, and Qin_30_1_398.7441 are in the same VIC location
Qin_28_1_270.358	-121.71625	47.86792	-121.71875	47.90625	Qin_28_1_270.358, Qin_25_1_293.3251, and Qin_30_1_398.7441 are in the same VIC location
Qin_30_1_398.7441	-121.73958	47.91208	-121.71875	47.90625	Qin_28_1_270.358, Qin_25_1_293.3251, and Qin_30_1_398.7441 are in the same VIC location
Qin_25_1_296.0115	-121.79625	48.36458	-121.78125	48.34375	
Qin_25_1_526.9275	-121.39542	47.71208	-121.40625	47.65625	Qin_25_1_526.9275 is in the same VIC location as Qin_31_1_304.1637
Qin_31_1_304.1637	-121.39625	47.66958	-121.40625	47.65625	Qin_25_1_526.9275 is in the same VIC location as Qin_31_1_304.1637
Qin_26_1_221.4949	-121.85208	47.82625	-121.84375	47.78125	

ID	Long	Lat	VIC Long	VIC_Lat	Notes
Qin_26_1_3.6896	-121.63792	47.88625	-121.59375	47.90625	Qin_31_1_473.6856 and Qin_26_1_3.6896 are in the same VIC location
Qin_31_1_473.6856	-121.64375	47.88042	-121.59375	47.90625	Qin_31_1_473.6856 and Qin_26_1_3.6896 are in the same VIC location
Qin_26_1_331.0489	-121.89375	47.56292	-121.90625	47.53125	
Qin_26_1_507.4592	-121.76958	48.15042	-121.71875	48.15625	
Qin_27_1_418.8577	-121.63125	48.22875	-121.65625	48.15625	
Qin_27_1_87.6569	-121.89625	47.93708	-121.84375	47.96875	
Qin_28_1_273.5458	-121.65042	47.97125	-121.59375	47.96875	
Qin_28_1_458.1675	-121.78792	47.70292	-121.71875	47.71875	
Qin_29_1_321.1701	-121.69625	47.86208	-121.65625	47.90625	
Qin_29_1_427.7249	-121.43792	47.83875	-121.40625	47.84375	Qin_29_1_427.7249 is in the same VIC location as Qin_38_1_360.4952
Qin_38_1_360.4952	-121.47125	47.85875	-121.40625	47.84375	Qin_29_1_427.7249 is in the same VIC location as Qin_38_1_360.4952
Qin_29_1_763.1644	-121.91292	48.27042	-121.90625	48.28125	
Qin_30_1_470.5383	-121.43792	47.70792	-121.46875	47.71875	Qin_39_1_278.4902 is in the same VIC location as Qin_30_1_470.5383
Qin_39_1_278.4902	-121.40875	47.72292	-121.46875	47.71875	Qin_39_1_278.4902 is in the same VIC location as Qin_30_1_470.5383
Qin_30_1_48.1626	-122.03458	47.89125	-121.96875	47.90625	
Qin_30_1_840.0352	-122.02125	48.12958	-122.03125	48.09375	
Qin_31_1_28.3423	-122.14292	48.01208	-122.15625	47.96875	Qin_31_1_28.3423 and Qin_32_1_19.5725 are in the same VIC location
Qin_32_1_19.5725	-122.13708	47.99708	-122.15625	47.96875	Qin_31_1_28.3423 and Qin_32_1_19.5725 are in the same VIC location
Qin_32_1_367.7221	-121.93042	48.28042	-121.96875	48.34375	
Qin_32_1_42.2623	-121.92125	47.58875	-121.96875	47.59375	Qin_33_1_61.6619 is in the same VIC location as Qin_32_1_42.2623
Qin_33_1_190.0174	-122.06292	48.17208	-122.03125	48.21875	
Qin_33_1_309.9808	-121.80458	47.79208	-121.78125	47.78125	Qin_33_1_309.9808 and Qin_34_1_404.0772 are in the same VIC location
Qin_34_1_404.0772	-121.79625	47.79292	-121.78125	47.78125	Qin_33_1_309.9808 and Qin_34_1_404.0772 are in the same VIC location
Qin_33_1_421.4683	-121.51375	47.75458	-121.53125	47.71875	Qin_40_1_249.4479 is in the same VIC location as Qin_33_1_421.4683
Qin_40_1_249.4479	-121.49625	47.76042	-121.53125	47.71875	Qin_40_1_249.4479 is in the same VIC location as Qin_33_1_421.4683
Qin_33_1_61.6619	-121.96208	47.59625	-121.96875	47.59375	Qin_33_1_61.6619 is in the same VIC location as Qin_32_1_42.2624
Qin_34_1_3.3934	-121.48625	47.79625	-121.40625	47.78125	Qin_34_1_3.3934 is in the same VIC location as Qin_41_1_2.0084

ID	Long	Lat	VIC Long	VIC_Lat	Notes
Qin_41_1_2.0084	-121.49625	47.78958	-121.40625	47.78125	Qin_34_1_3.3934 is in the same VIC location as Qin_41_1_2.0084
Qin_34_1_79.3178	-121.91375	47.87125	-121.90625	47.96875	Qin_35_1_105.4906 and Qin_34_1_79.3178 are in the same VIC location
Qin_35_1_105.4906	-121.87958	47.90458	-121.90625	47.96875	Qin_35_1_105.4906 and Qin_34_1_79.3178 are in the same VIC location
Qin_35_1_30.7617	-122.03875	47.99625	-122.09375	48.03125	
Qin_36_1_177.2956	-121.83792	47.55375	-121.78125	47.59375	Qin_37_1_258.6796 is in the same VIC location as Qin_36_1_177.2956
Qin_37_1_258.6796	-121.79542	47.57125	-121.78125	47.59375	Qin_37_1_258.6796 is in the same VIC location as Qin_36_1_177.2956
Qin_36_1_36.5215	-122.06125	48.02292	-122.09375	48.09375	
Qin_36_1_370.5385	-121.63708	48.28625	-121.65625	48.34375	
Qin_37_1_881.3598	-121.71292	48.07542	-121.65625	48.09375	
Qin_38_1_185.0463	-122.04625	48.35125	-122.03125	48.34375	
Qin_39_1_429.0749	-121.82125	48.36792	-121.84375	48.34375	
Qin_40_1_532.0297	-121.83958	48.14792	-121.78125	48.15625	
Qin_40_1_796.691	-121.77958	48.28375	-121.71875	48.28125	
Qin_41_1_19.5162	-122.32931	48.35431	-122.28125	48.34375	Outside of the Snohomish River. Part of the Skagit River basin.
Qin_41_1_243.9706	-121.91458	48.20292	-121.90625	48.21875	Qin_41_1_243.9706 and Qin_50_1_226.5634 are in the same VIC location
Qin_50_1_226.5634	-121.93042	48.21208	-121.90625	48.21875	Qin_41_1_243.9706 and Qin_50_1_226.5634 are in the same VIC location
Qin_41_1_960.4984	-121.94542	48.10375	-121.90625	48.09375	
Qin_42_1_154.0936	-122.16208	48.30125	-122.15625	48.34375	
Qin_42_1_380.5413	-121.74792	48.20042	-121.71875	48.21875	
Qin_43_1_298.6373	-121.67208	48.26792	-121.65625	48.21875	
Qin_43_1_477.828	-121.95458	48.36292	-121.90625	48.34375	
Qin_44_1_262.0068	-121.96458	48.11458	-121.90625	48.15625	
Qin_45_1_269.3813	-121.99708	48.21292	-121.96875	48.21875	
Qin_45_1_765.2604	-121.70458	48.27375	-121.65625	48.28125	
Qin_46_1_357.6096	-121.79542	48.26875	-121.84375	48.21875	
Qin_46_1_803.0399	-121.77792	48.08958	-121.71875	48.09375	
Qin_47_1_157.9805	-122.09792	48.34125	-122.09375	48.34375	

ID	Long	Lat	VIC Long	VIC_Lat	Notes
Qin_48_1_434.725	-121.88042	48.37958	-121.84375	48.40625	
Qin_49_1_248.3835	-121.89625	48.12625	-121.84375	48.15625	
Qin_51_1_406.2031	-121.80208	48.23292	-121.78125	48.21875	
Qin_7_1_861.9765	-121.50458	47.53708	-121.46875	47.53125	
Qin_8_1_427.6026	-121.86292	48.03125	-121.84375	48.03125	
Qin_9_1_403.0672	-121.33792	47.88792	-121.34375	47.90625	